Sediment characteristics and microbial mats in a marine mangrove, Manche-à-eau lagoon (Guadeloupe)

Swanne Gontharet, Antoine Crémière, Marie-Madeleine Blanc-Valleron, Mathieu Sebilo, Olivier Gros, Anniet M. Laverman, et al.

Journal of Soils and Sediments

ISSN 1439-0108

J Soils Sediments
DOI 10.1007/s11368-016-1555-6

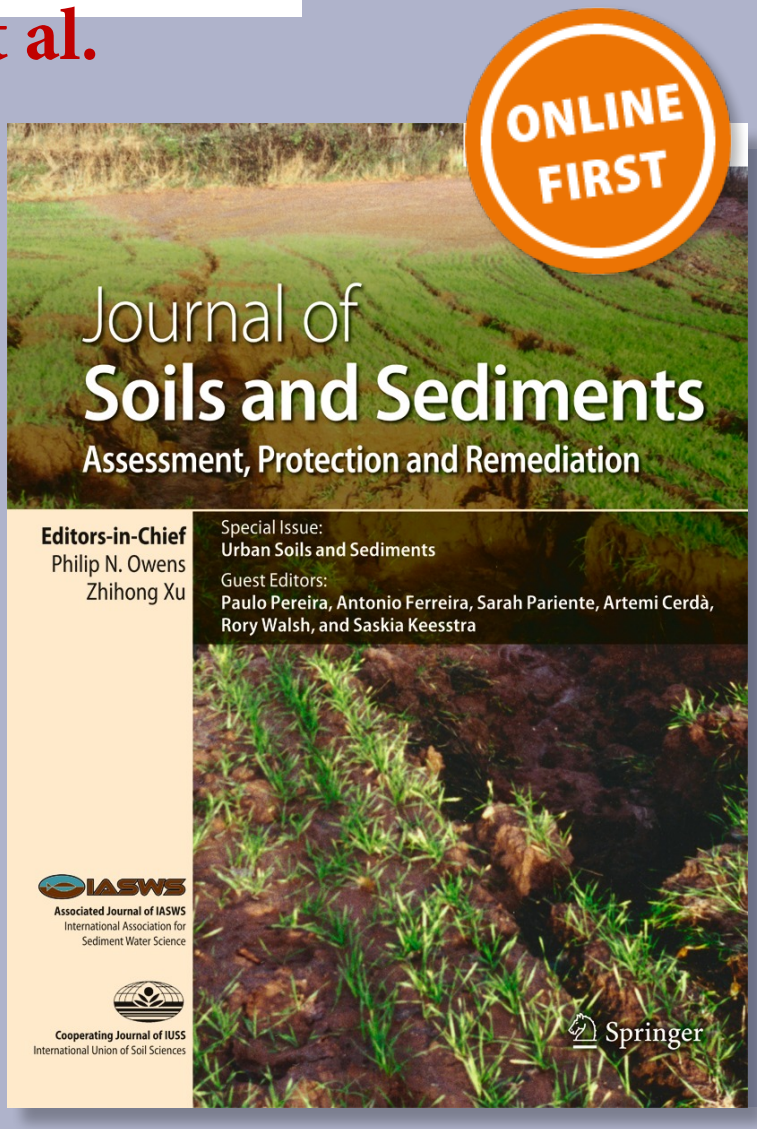

Springer

J Soils Sediments
DOI 10.1007/s11368-016-1555-6

ISEB 2015: BIOGEOCHEMICAL DYNAMICS OF SEDIMENT-WATER SYSTEMS: PROCESSES AND MODELLING

Sediment characteristics and microbial mats in a marine mangrove, Manche-à-eau lagoon (Guadeloupe)

Swanne Gontharet[1] · **Antoine Crémière**[2] · **Marie-Madeleine Blanc-Valleron**[3] · **Mathieu Sebilo**[4] · **Olivier Gros**[5] · **Anniet M. Laverman**[6] · **David Dessailly**[1]

Received: 3 March 2016 / Accepted: 7 September 2016

Abstract
Purpose Marine mangrove sediments in the Manche-à-Eau lagoon (Guadeloupe, Caribbean Sea) harbor locally extensive, white microbial mats. These mats cover the surface of reduced sediments near the roots of red mangrove trees, *Rhizophora mangle*, and are mainly composed of sulfur-oxidizing bacteria belonging to the *Beggiatoaceae* family, with some filamentous cyanobacteria. The goal of this study was to investigate the possible influence of sediment characteristics on the presence of these microbial mats.
Materials and methods Four push cores were collected in April 2013, two from zones with microbial mats and two from zones without mats. Sediment characteristics (grain-size distribution, mineralogy, total organic carbon (TOC) and total nitrogen (TN) contents, atomic TOC/TN ratios, and organic matter (OM) $\delta^{13}C$ values) were compared for all four cores.
Results and discussion Significant differences were observed between sediments below microbial mats and those without mats. Sediments with microbial mats contained greater amounts of clay, and higher TOC, TN, and TOC/TN ratios, with lower total carbonate content and $\delta^{13}C$ values. The higher clay content most likely results from lower fluid flow velocity near to mangrove roots, while higher TOC/TN ratios and lower $\delta^{13}C$ values indicate higher inputs of OM from mangrove trees. These results are consistent with the fact that microbial mats were observed near the roots of mangrove trees, which trap OM from terrestrial vegetation and fine sediments.
Conclusions The grain-size distribution of sediment particles, the total carbonate content, and the $\delta^{13}C$ values are the main parameters discriminating between zones with microbial mats and those without mats. Variations in total carbonate content, which is mainly of biogenic origin, result from conditions that are more favorable for benthic organisms in zones without microbial mats. Variations of the TOC/TN ratios are controlled by the presence of a non-negligible amount of inorganic nitrogen bound to surface clay mineral particles and/or by microbial processes.

Keywords Atomic TOC/TN ratios · Grain size · Mineralogy · Organic matter sources · Stable carbon isotopes

Responsible editor: Nives Ogrinc

✉ Swanne Gontharet
swanne.gontharet@univ-littoral.fr

[1] Laboratoire d'Océanologie et de Géosciences, CNRS UMR 8185 LOG, Université Lille Nord de France COMUE, Université du Littoral-Côte d'Opale (ULCO), 32 Avenue Foch, 62930 Wimereux, France

[2] Geological Survey of Norway (NGU), P.O. 6315, Sluppen, 7491 Trondheim, Norway

[3] CR2P, UMR 7207, Muséum National d'Histoire Naturelle, Sorbonne Universités - MNHN, CNRS, UPMC-Paris 6, 57 rue Cuvier, 75231 Paris Cedex 05, France

[4] Institute of Ecology and Environmental Sciences (IEES), Sorbonne Universités, CNRS, UPMC University Paris 06, 4 Place Jussieu, 75005 Paris, France

[5] Institut de Biologie Paris-Seine UMR 7138-Evolution Paris-Seine, Equipe Biologie de la Mangrove, Université des Antilles, BP 592, 97159 Point-à-Pitre Cedex, Guadeloupe, France

[6] Ecobio, UMR 6553, Université de Rennes 1, Campus de Beaulieu, 263 Avenue du Général Leclerc, 35042 Rennes Cedex, France

1 Introduction

Mangrove forests, predominant in the intertidal zone of tropical and subtropical coastlines, are highly productive ecosystems that efficiently trap material suspended in the water

Published online: 11 October 2016

column (Jennerjahn and Itterkkot 2002; Adame et al. 2010). Sediments in such environments receive higher organic matter (OM) inputs, remineralized to a large extent by microbially mediated processes, leading to nutrient regeneration (Bouillon et al. 2008). Microbial activity is thus crucial for these coastal ecosystems, playing a key role in carbon and nutrient cycling. Complex dynamic ecosystems may develop at the sediment-water interface, forming microbial mats, often observed in shallow habitats (e.g., Canfield and Des Marais 1993; Al-Thukair et al. 2007; Delfino et al. 2012).

Microbial mats typically have a community structure driven by vertical micro-gradients of oxygen, hydrogen sulfide, and light (e.g., van Gemerden 1993; Meysman et al. 2015). These thin-layered structures are composed not only of phototrophic, heterotrophic, and chemolithoautotrophic bacteria but also of archaea and eukaryotic microalgae (Stolz 2000). The extracellular polymeric substance (EPS), principally produced by oxygenic phototrophic cyanobacteria (Decho 1990), may potentially be a structuring agent in microbial mats and may also enhance sediment stabilization and resistance to erosion (Stal 2010).

Microbial mats are characterized by a wide range of metabolic processes resulting in coupled reactions; primary production by cyanobacteria fuels the metabolism of sulfate-reducing bacteria, and the resulting sulfide is then oxidized by anoxygenic phototrophic bacteria and by colorless sulfur bacteria. Studying these unique ecosystems can lead to better understanding of biogeochemical cycles (C, N, S) and their interactions (Canfield and Des Marais 1993; Seckbach and Oren 2010). The influence of environmental (hydrological conditions) and physicochemical factors (light, temperature, salinity, pH, oxygen, and electron donor acceptors) on the structure and dynamics of modern microbial mats has been extensively studied (e.g., Al-Thukair et al. 2007; Seckbach and Oren 2010; Delfino et al. 2012), but the influence of sedimentary parameters (grain-size distribution, mineralogy, and OM geochemistry) remains largely unexplored. Extensive white microbial mats have recently been identified at the edge of the Manche-à-Eau lagoon colonized by mangrove trees (Guadeloupe, Lesser Antilles, French West Indies; Fig. 1a, b). Push cores from this Caribbean lagoon were therefore studied to identify the sedimentary characteristics of zones at the sediment-water interface where microbial mats have developed, in comparison with sediments from zones without mats.

2 Materials and methods

2.1 Study sites and field sampling

The Manche-à-Eau lagoon (16° 15′ N, 61° 35′ W), covering an area of 0.26 km^2, is located on the northern coast of the Guadeloupe archipelago, in the French West Indies (Fig. 1a). It is linked to the Grand Cul-de-Sac Marin lagoon by a narrow sea channel, the Rivière Salée, which separates the volcanic island of Basse-Terre and the limestone-dominated island of Grande-Terre (Guilcher and Marec 1978; Fig. 1a). Guadeloupe has a humid tropical climate, with a dry season from December to May and a rainy season from June to November. The annual average air temperature ranges from 20 to 31 °C, and the annual rainfall ranges from 1500 to 1800 mm yr^{-1}.

This shallow, semiclosed marine lagoon is elongated (reaching 910 m long and 425 m wide) with a maximum water depth of 2 m (Mantran et al. 2009). It is fringed by red mangrove trees, *Rhizophora mangle*, and flooded continuously. The white mats recently observed at the sediment-water interface in several locations around the lagoon are composed of colorless filamentous free-living sulfur-oxidizing bacteria, belonging to two new species (*Candidatus* Isobeggiatoa and *Candidatus* Maribeggiatoa) of the *Beggiatoaceae* family (Jean et al. 2015; Fig. 1b). Some filamentous cyanobacteria belonging to the *Oscillatoriales* family (Guidi-Rontani et al. 2014) has also been observed within the *Beggiatoa* mats.

Water circulation is slow and complex, driven by the interaction between southeasterly trade-wind currents, semidiurnal tidal flow, and continental freshwater inflow. Mantran et al. (2009) calculated a water renewal rate of 14.8 % at each tide, by estimating the mean volume of input and output water during the flood and ebb tides. This high renewal rate, associated with active hydrodynamism, results in well-mixed, homogeneous lagoon water (Mantran et al. 2009). Water temperature (~28 °C) and salinity (~35 ‰) are relatively constant below 0.5 m depth (Pascal et al. 2014). Tidal periodicity is semidiurnal and the tidal amplitude in the lagoon oscillates between 30 and 40 cm (tide gauge of Pointe-à-Pitre, REFMAR®).

Sampling was carried out in April 2013, during the dry season. Sediment samples were collected from four sites in the Manche-à-Eau lagoon, in water depths of 0.5 m (Fig. 1c). At each site, one plastic core tube (70 mm in diameter and 60 cm long) was manually pushed into the sediment, during low tide, by snorkeling. Cores A (16° 16′ 33.75″ N, 61° 33′ 18.07″ W) and B (16° 16′ 33.44″ N, 61° 33′ 17.69″ W) were collected from sites 1.4 m apart, in the zone characterized by the presence of microbial mats, while cores C (16° 16′ 33.72″ N, 61° 33′ 18.06″ W) and D (16° 16′ 33.73″ N, 61° 33′ 18.04″ W) were collected from the zone not colonized by *Beggiatoa*, 0.2 m from core A and 1.3 m from core B.

Sedimentation rates determined using the ^{210}Pb technique on three of the cores (A, B, and C) ranged from 0.91 to 1.0 cm yr^{-1} (Crémière et al. submitted). As measured under mesocosm conditions by Jean et al. (2015), dissolved sulfide concentrations in the top 5 mm-depth sediments were generally higher in sediments collected below microbial mats (from ca. 1 to 8 mM) than in uncolonized sediments (ca. 1 mM).

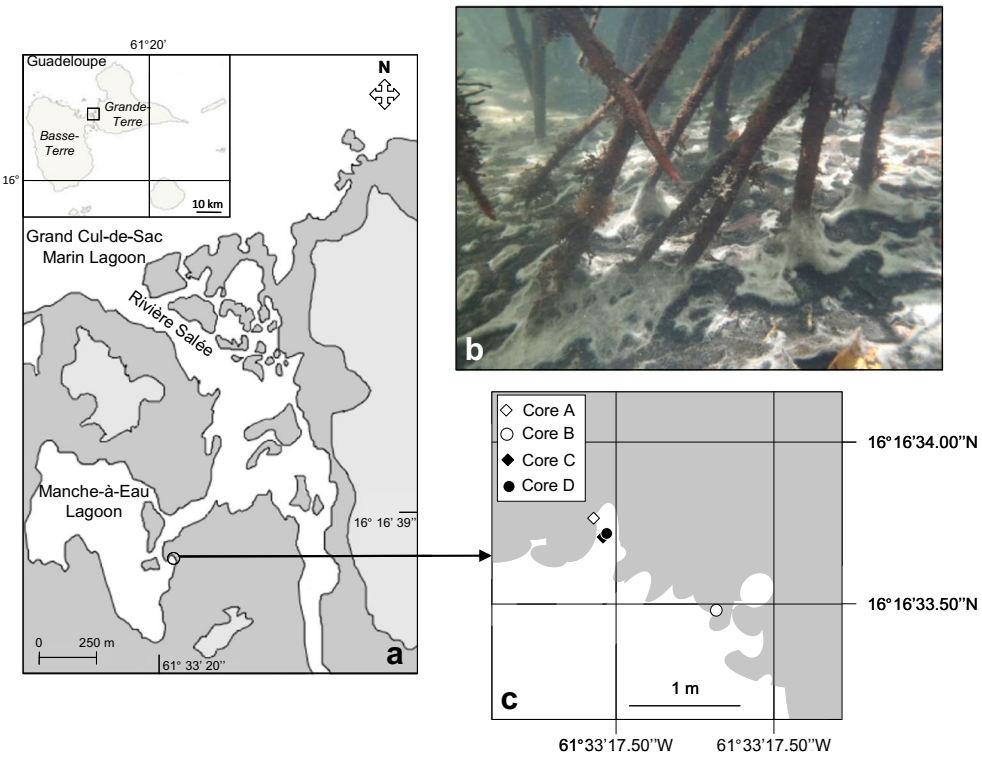

Fig. 1 **a** Map showing the Manche-à-Eau lagoon and its connection to the Grand Cul-de-Sac Marin lagoon. **b** Underwater picture of patches of white microbial mats on the *R. mangle* mangrove sediments. **c** Schematic representation showing the position of the sampling sites

In the laboratory, each core was sliced into ~5 cm layers. Each of the resulting slices was then divided into two subsamples; one of which was kept wet for grain-size analysis, while the other was frozen at -20 °C, lyophilized, and stored until required for analysis to investigate mineralogy and OM geochemistry.

2.2 Laboratory analysis

Grain-size analysis from 0.375 to 2000 μm for all wet samples used a Particle Size Analyzer Beckman-Coulter™ LS 230 (gallium arsenide, 750 nm wavelength; Brea, USA). The coarse fraction (>2000 μm) of all samples was removed by wet sieving prior to analysis; it was mainly composed of mangrove vegetation debris and carbonate shells. One subsample from each core and depth was treated by ultrasounds to disrupt aggregation structures prior to grain-size analysis. Another subsample was left in a natural state for aggregate analysis. All samples were analyzed in triplicate, and the relative error of triplicate samples was less than 3 %. In all grain-size distributions obtained with and without treatment, particle size classes were assigned according to the Wentworth (1922) grain-size scale, 0.2–4.0 μm for the clay fraction, 4.0–62.5 μm for the silt fraction, and 62.5–2000 μm for the sand fraction. In all grain-size distributions obtained without treatment, the following three different aggregate sizes were used: clay/silt fraction (<62.5 μm), micro-aggregates (62.5–250 μm), and small macro-aggregates (250–2000 μm). For each site and depth, the difference was calculated between the relative percentages of each size fraction obtained after ultrasonic treatment and those obtained without treatment. The positive values indicated the sizes and the relative percentages of particles involved in aggregation structure.

The total carbonate content of bulk sediments, expressed as dry sediment weight (wt.%), was determined using a manual calcimeter (OFITE, Houston, USA) calibrated with pure carbonate. It was estimated by reaction of 100 mg of fine powdered sediment with 0.4 cm^3 of HCl 8 N, with an absolute error of 1 %. Mineral composition was identified by X-ray powder diffraction (XRD) on dried ground sediment subsamples. Measurements were run on a D2 Phaser X-ray diffractometer (Cu Kα, Ni-filtered, radiation; Bruker AXS instrument, Kalsruhe, Germany), scanning 2°–64° 2θ at a rate of 0.02° 2θ per second. The main mineral phases were identified using the DIFFRAC.SUITE EVA v4 software. This identification was coupled with observation of dried bulk sediments using a Stemi 2000 ZEISS stereomicroscope.

Total organic carbon (TOC) and total nitrogen (TN) were measured in bulk sediments using a Vario EL III elemental analyzer (Elementar, Hanau, Germany). Before analysis, freeze-dried sediments were finely ground in an agate mortar and homogenized. They were then acidified with 1 M HCl to remove carbonates, washed with distilled water, centrifuged until a pH of ~7 was reached, and dried at 40 °C overnight. Uncertainties on these measurements were 0.14 % for TOC and 0.02 % for TN. In this study, the TOC/TN ratio refers to the atomic ratio, which is obtained by multiplying the weight TOC/TN ratio with the (nitrogen atomic mass (14.0067)/carbon atomic mass (12.0107)) ratio.

Stable carbon isotopes were determined in an aliquot of each carbonate-free sample by thermal decomposition in an Elemental Analyzer (Elementar, Hanau, Germany) coupled to a continuous-flow isotope ratio mass spectrometer (Isoprime, Manchester, UK). Carbon isotope values were expressed in the usual δ notation, which was determined as

$$\delta^{13}C = \left[\frac{R_{sample}}{R_{standard}} - 1\right] \times 1000$$

where R is the isotopic ratio ($^{13}C/^{12}C$). The international standard is Vienna Pee Dee Belemnite for carbon with a $^{13}C/^{12}C$ ratio of 0.01112372. Calibrations used various international and laboratory standards for carbon and nitrogen, cellulose (IAEA-CH-3 $\delta^{13}C$ = -24.724 ‰) and caffeine (IAEA-600 $\delta^{13}C$ = -27.771 ‰). Tyrosine ($\delta^{13}C$ = -23.2 ‰, laboratory standard) was used to ensure the accuracy and precision of the isotopic compositions obtained. Analytical precision was about ± 0.1 ‰ for $\delta^{13}C$.

2.3 Statistical analysis

The mean and standard deviation of the sediment parameters were calculated from the values obtained for the two sediment cores collected within each zone. Five statistical parameters were calculated from the grain-size distribution of untreated sediments using the GRADISTAT software (Blott and Pye 2001) to characterize their variability, following the Folk and Ward (1957) graphical method, mode (the most abundant grain-size class), mean (the weighted average grain-size class), sorting (the spread of sizes around the average), and skewness (the symmetry or preferential spread to one side of the average). Correlations between grain size and OM geochemical characteristics were assessed by applying Pearson's correlation tests combined with Student's t tests (n = 10). The test results were reported with a confidence level of 95 or 99 % (P values of 0.05 and 0.01, respectively). Principal component analysis (PCA), a multivariate analytical tool, was used to study the relationship of the sedimentary parameters measured to highlight their similarities and differences. All statistical analyses used the free R statistical software (version 2.14.1).

3 Results

3.1 Comparison of the four sediment cores

Cores A and B, collected from sites 1.4 m apart, were remarkably similar in appearance, with black peat-like sediment in the first 20 cm and dark brown sediment below this depth. In contrast, cores C and D were characterized by homogeneous dark brown sediment and also contained several worm burrows (*Arenicola brasiliana*).

For each core, results for grain-size distribution, mineralogical composition, and OM characteristics are shown in Table 1. All sediments studied corresponded to sandy silt or silt (Folk's sediment classification method; Folk 1954), characterized by predominance of the silt fraction (65–82 %), associated with sand (9–28 %) and clay (4–14 %). The only sand fraction observed in all cores was fine sand grains (63–250 μm).

The XRD patterns of the sediments revealed the presence of calcium carbonate, pyrite, and clay minerals (mostly halloysite and kaolinite) associated with minor amounts of quartz, cristobalite, and feldspars (Fig. 2a). The total calcium carbonate content showed great variation, ranging from 7 to 70 %. Aragonite (35 to 93 % of the total carbonate content) and stoichiometric calcite (6 to 62 % of the total carbonate content) were the dominant carbonate phases. These two carbonate phases were sometimes associated with minor quantities of magnesium calcite (0 to 9 % of the total carbonate content). Morphological observations of sediments showed that these carbonates originated predominantly from numerous biogenic elements (Fig. 2b). The sieved fraction was mainly composed of fragments of aragonitic green algae *Halimeda*, together with other calcareous remains of bivalves and gastropods (mainly aragonitic shells of *Caecum* species; Fig. 2c). Minor amounts of benthic foraminiferal tests, sea urchin spicules, and ostracod valves were also observed. Pyrite was associated with debris of ligneous organic components (mostly from mangrove trees), as well as biogenic carbonate elements.

The TOC content in sediment samples ranged from 4.9 to 19.8 %, while the TN content ranged from 0.3 to 1.4 %. The plot of TOC versus TN contents illustrates a strong positive correlation between these two parameters (Pearson's correlation coefficient, r = 0.954, n = 10, P < 0.01). The interception of the linear correlation between TOC and TN contents, with a slightly positive value of 0.0356, reveals the presence of a non-negligible amount of inorganic nitrogen in sediments (Goñi et al. 1998). Sedimentary $[TOC/TN]_{atomic}$ ratios for all four sediment cores ranged from 13.8 to 23.7, and $\delta^{13}C$ values ranged from -26.7 to -24.4 ‰.

PCA was used to evaluate the relationships between sediment characteristics (clay and sand percentages, total carbonate contents, $[TOC/TN]_{atomic}$ ratios, and OM $\delta^{13}C$) for all four cores (Fig. 3). The first two factors explained 86.7 % of the total variance. Factor 1, with 64 % of the variance, grouped all clay and sand percentages, total carbonate contents, and OM $\delta^{13}C$ values. Factor 2, representing 22.7 % of the variance, grouped $[TOC/TN]_{atomic}$ ratios. While factor 2 separated the superficial sediments from the deeper sediments, for all four cores, factor 1 divided the sediment samples into two separate groups, based on the presence or absence of microbial mats.

Thus, the factors used to discriminate between zones with microbial mats and those without mats are clay and sand percentages, total carbonate content, and OM $\delta^{13}C$ values. Therefore, in the following sections, results are presented by zone type,

Table 1 Mean physicochemical characteristics (grain-size percentages, total carbonate contents, and OM geochemical parameters) for the four cores

	Mean depth (cm)	Particle-size distribution (%)			Total carbonate content (%)	TOC (%)	TN (%)	Atomic TOC/TN ratio	$\delta^{13}C_{org}$ (‰)
		Clay	Silt	Sand					
Core A	2.5	11.0 ± 2.0	76.4 ± 2.1	12.7 ± 0.1	10 ± 0	18.7 ± 1.2	1.4 ± 0.0	16.0 ± 1.0	-26.4 ± 0.3
	7.5	12.9 ± 1.1	76.4 ± 0.1	10.7 ± 1.2	11 ± 0	17.5 ± 0.2	1.2 ± 0.0	17.4 ± 0.7	-26.3 ± 0.1
	12.5	12.5 ± 1.2	74.6 ± 0.8	12.9 ± 2.0	14 ± 2	16.5 ± 1.1	1.1 ± 0.0	17.5 ± 1.4	-25.7 ± 0.3
	17.5	10.0 ± 0.1	69.0 ± 0.1	21.0 ± 0.2	13 ± 3	17.6 ± 0.3	1.1 ± 0.1	19.0 ± 1.4	-25.6 ± 0.1
	22.5	10.1 ± 1.7	68.6 ± 3.9	21.3 ± 5.6	11 ± 2	17.3 ± 0.3	1.1 ± 0.0	19.3 ± 1.0	-25.4 ± 0.0
		11.3 ± 1.8	**73.0 ± 4.0**	**15.7 ± 5.3**	**12 ± 2**	**17.5 ± 1.0**	**1.2 ± 0.1**	**15.9 ± 1.3**	**-25.9 ± 0.4**
Core B	2.5	12.8 ± 0.4	77.8 ± 2.3	9.4 ± 0.3	12 ± 5	17.8 ± 1.1	1.2 ± 0.1	17.6 ± 2.0	-25.9 ± 0.2
	7.5	11.7 ± 0.8	70.2 ± 1.0	18.1 ± 1.8	13 ± 2	16.9 ± 0.8	1.1 ± 0.0	18.6 ± 1.2	-25.7 ± 0.2
	12.5	13.8 ± 0.4	76.0 ± 2.3	10.3 ± 0.3	21 ± 5	15.1 ± 1.0	1.0 ± 0.1	18.6 ± 1.9	-25.6 ± 0.1
	17.5	13.5 ± 0.2	69.6 ± 2.1	16.9 ± 0.5	23 ± 11	13.9 ± 1.9	0.9 ± 0.1	19.1 ± 4.1	-25.4 ± 0.0
	22.5	7.2 ± 0.1	75.6 ± 0.8	17.1 ± 0.9	27 ± 10	13.5 ± 1.7	0.8 ± 0.1	19.8 ± 3.9	-25.6 ± 0.1
		11.8 ± 2.4	**73.8 ± 3.8**	**14.4 ± 3.8**	**19 ± 9**	**15.4 ± 2.1**	**1.0 ± 0.2**	**17.7 ± 2.3**	**-25.6 ± 0.2**
Core C	2.5	4.5 ± 0.2	76.9 ± 0.4	18.6 ± 0.6	19 ± 0	13.7 ± 0.0	1.1 ± 0.0	14.4 ± 0.0	-25.2 ± 0.0
	7.5	4.4 ± 0.0	72.7 ± 0.3	22.9 ± 0.3	19 ± 0	14.2 ± 0.0	1.2 ± 0.0	13.8 ± 0.0	-25.2 ± 0.0
	12.5	5.0 ± 0.2	72.6 ± 0.9	22.4 ± 1.1	42 ± 0	10.1 ± 0.0	0.7 ± 0.0	17.3 ± 0.0	-25.0 ± 0.0
	17.5	5.3 ± 0.2	73.8 ± 0.4	20.9 ± 0.5	47 ± 0	8.8 ± 0.0	0.6 ± 0.0	17.4 ± 0.0	-24.9 ± 0.0
	22.5	6.0 ± 0.3	70.1 ± 0.1	24.0 ± 0.2	69 ± 1	4.9 ± 0.0	0.3 ± 0.0	16.7 ± 0.0	-24.4 ± 0.0
		5.0 ± 0.6	**73.2 ± 2.3**	**21.8 ± 2.0**	**39 ± 19**	**10.3 ± 3.4**	**0.8 ± 0.3**	**13.7 ± 1.3**	**-24.9 ± 0.3**
Core D	2.5	4.2 ± 0.1	79.9 ± 2.4	15.9 ± 0.5	17 ± 0	13.9 ± 0.0	1.1 ± 0.0	15.2 ± 0.0	-24.9 ± 0.0
	7.5	4.9 ± 0.1	72.9 ± 2.2	22.2 ± 0.7	28 ± 0	12.3 ± 0.0	0.9 ± 0.0	16.7 ± 0.0	-25.0 ± 0.0
	12.5	5.3 ± 0.2	73.1 ± 2.2	21.6 ± 0.6	44 ± 0	8.6 ± 0.0	0.6 ± 0.0	16.7 ± 0.0	-24.7 ± 0.0
	17.5	4.0 ± 0.1	73.1 ± 2.2	22.9 ± 0.7	33 ± 0	11.7 ± 0.0	0.8 ± 0.0	17.7 ± 0.0	-25.0 ± 0.0
	22.5	5.5 ± 0.4	69.0 ± 2.4	25.5 ± 2.6	68 ± 1	5.2 ± 0.0	0.3 ± 0.0	17.8 ± 0.0	-24.9 ± 0.0
		4.8 ± 0.6	**73.6 ± 4.2**	**21.6 ± 3.4**	**38 ± 17**	**10.3 ± 3.1**	**0.7 ± 0.2**	**14.4 ± 0.8**	**-24.9 ± 0.1**

Bold data are the average value

classified as "with microbial mats" combining the results for cores A and B (zone AB) and "without mats," combining results for cores C and D (zone CD).

3.2 Comparison of the two zones (zone AB, with microbial mats, and zone CD, without mats)

Results for grain-size distribution show that, while silt content was roughly the same for both zones (mean 73 ± 4 %), zone AB, below microbial mats, had a higher clay content and generally lower sand fraction than zone CD, without microbial development (Table 1). The mean grain size (MGS) was therefore lower in zone AB (20.8 ± 3.0 μm) than in zone CD (27.1 ± 1.4 μm) (Table 2). Furthermore, sediments below microbial mats were poorly sorted (sorting 2.9 to 3.4) and displayed a tri- or poly-modal distribution (Fig. 4a), with a tailing effect skewing towards the fine-grained end (skewness -0.31 to -0.17) except for 22.5 cm depth (skewness -0.07 ± 0.02) (Table 2). Sediments without microbial mats are characterized by lower values of sorting (2.6 to 3.0), a uni- or bi-modal (major mode at 34.6–38 μm, corresponding to coarse silt; Fig. 4b) symmetrical distribution (skewness -0.09 to -0.03) (Table 2).

Between 6 and 29 % of the sedimentary particles, especially clay- to coarse silt-sized particles, were involved in the formation of aggregates (Table 2 and Fig. 5). Higher percentages of aggregated particles were observed in the zone with microbial mats (21 ± 5 %) than in the zone without microbial development (12 ± 3 %) in the first 15 cm of depth. Figure 5 also shows predominance of clay/silt-sized aggregates, representing 60 to 76 % of the total aggregates. Varying amounts of micro-aggregates (24–33 %) and macro-aggregates (0–13 %) were also observed.

Mineralogical composition showed no variation between zones or depths, except for clay minerals and carbonates. While clay minerals were more abundant in sediments from zone AB (below mats), lower abundances in carbonates were observed in those sediments (12 ± 3 %) than in sediments from zone CD (without mats) (39 ± 18 %) (Fig. 6). In both zones, higher percentages of aragonite were observed in deeper sediments, while total calcite content showed higher values at 7.5 cm depth.

At all depths, TOC and TN contents were generally characterized by higher values in sediments from zone AB, below microbial mats (TOC = 16.5 ± 2.0 %; TN = 1.1 ± 0.2 %) than

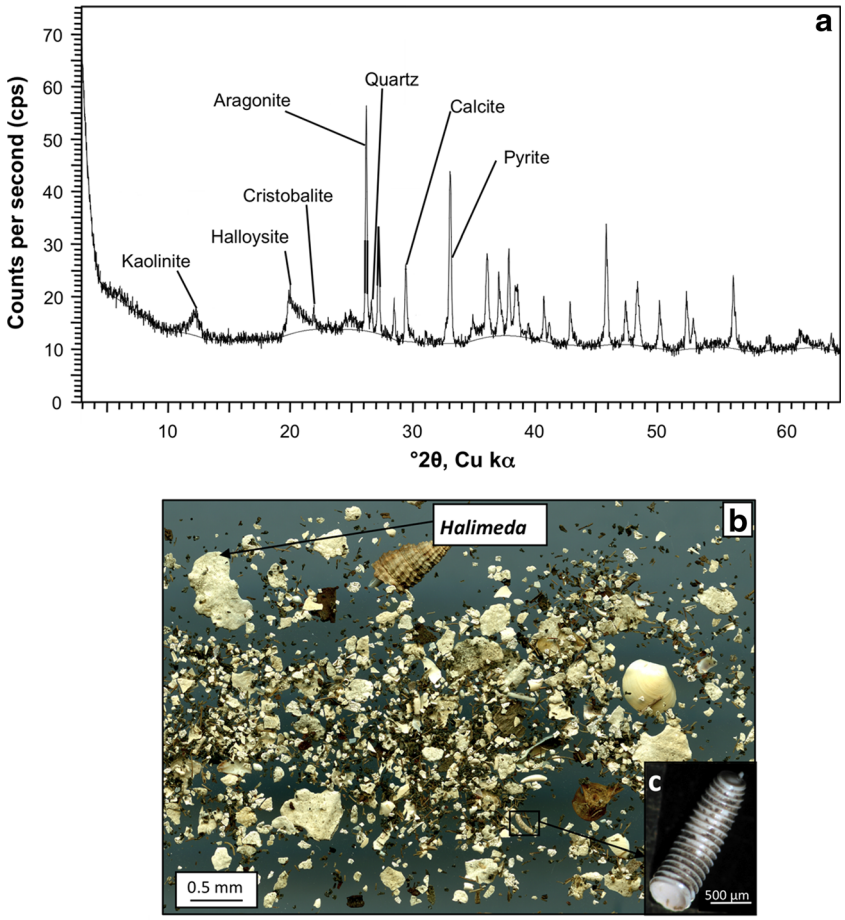

Fig. 2 **a** An example of a X-ray diffractogram (core D, 15 cm depth) with the main observed diffraction peak intensities in a sediment from the Manche-à-Eau lagoon. **b** The >250 µm sieved fraction of sediment (core C at 10 cm depth). Carbonates correspond to numerous green algae *Halimeda* fragments and to some shells of mollusks; *brown fragments* correspond to OM remains. **c** Close-up of a gastropod belonging to *Caecidae* family

from zone CD, not colonized by microbial mats (TOC = 10.3 ± 3.3 %; TN = 0.8 ± 0.3 %) (Table 1). There was, however, a decreasing trend with depth, in particular for sediments not colonized by microbial mats (zone CD). At all

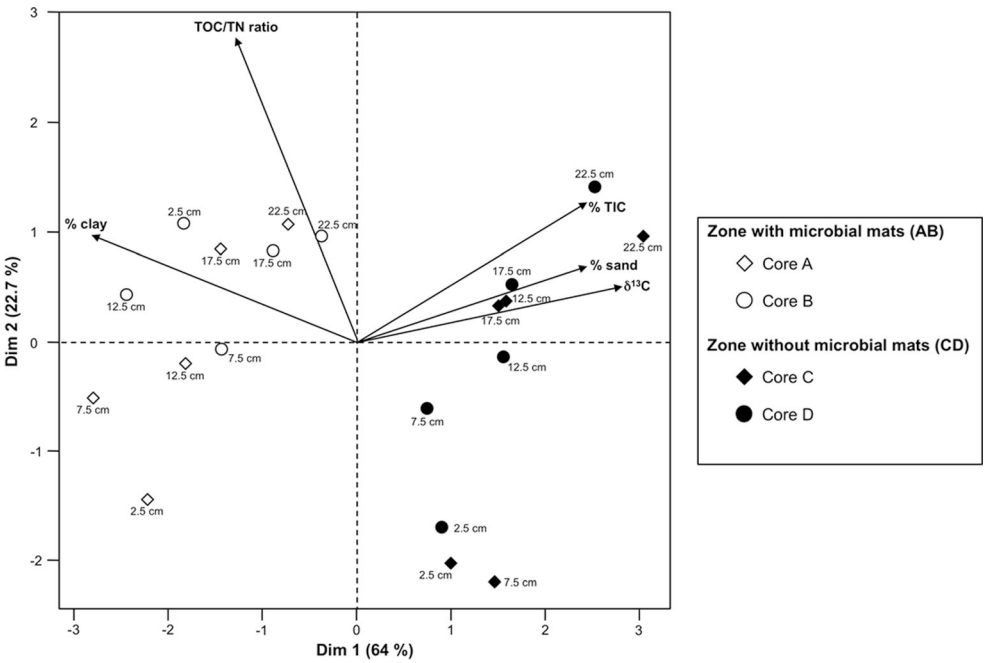

Fig. 3 Bi-dimensional rotated plot of factor 1 and factor 2 obtained by factor analysis for 20 samples (from two cores collected in each zone), using data for percentages of clay, sand, and total carbonate contents as well as the $[TOC/TN]_{atomic}$ ratios and $\delta^{13}C$ values

Table 2 Mean and standard deviation (SD) of the grain-size parameters and percentage of aggregated particles for the two zones

	Mean depth (cm)	Distribution type	Mean (μm)	Sorting	Skewness	Kurtosis	Aggregated particles (%)
Zone with microbial mats (zone AB)	2.5	Polymodal	19.3 ± 2.4	3.0 ± 0.1	-0.25 ± 0.06	0.93 ± 0.06	27 ± 2
	7.5	Polymodal	19.1 ± 2.3	3.3 ± 0.1	-0.21 ± 0.03	0.90 ± 0.03	15 ± 2
	12.5	Polymodal	18.3 ± 1.9	3.1 ± 0.0	-0.23 ± 0.06	0.90 ± 0.03	22 ± 2
	17.5	Polymodal	24.6 ± 0.4	3.3 ± 0.1	-0.26 ± 0.04	0.98 ± 0.06	18 ± 1
	22.5	Trimodal	22.5 ± 0.1	3.0 ± 0.0	-0.07 ± 0.02	0.95 ± 0.02	9 ± 2
			20.8 ± 3.0	**3.2 ± 0.2**	**-0.20 ± 0.08**	**0.94 ± 0.05**	**18 ± 6**
Zone without microbial mats (zone CD)	2.5	Unimodal	25.3 ± 0.6	2.7 ± 0.1	-0.07 ± 0.02	0.98 ± 0.01	13 ± 2
	7.5	Bimodal	28.3 ± 0.5	2.9 ± 0.0	-0.06 ± 0.01	0.96 ± 0.00	9 ± 3
	12.5	Unimodal	27.2 ± 0.8	2.9 ± 0.0	-0.06 ± 0.01	0.96 ± 0.01	15 ± 1
	17.5	Unimodal	27.0 ± 1.3	2.9 ± 0.1	-0.07 ± 0.01	0.96 ± 0.00	16 ± 3
	22.5	Bimodal	27.8 ± 1.5	3.1 ± 0.1	-0.05 ± 0.02	0.92 ± 0.01	8 ± 2
			27.1 ± 1.4	**2.9 ± 0.2**	**-0.08 ± 0.05**	**0.96 ± 0.02**	**12 ± 4**

Bold data are the average value

depths, sediments below microbial mats (zone AB) were mostly characterized by higher TOC/TN ratios and lower $\delta^{13}C$ values (Table 1). Significant differences in TOC/TN ratios and $\delta^{13}C$ values were observed with depth.

4 Discussion

Differences in grain-size distributions between the two zones indicate variations in sedimentation environments, including

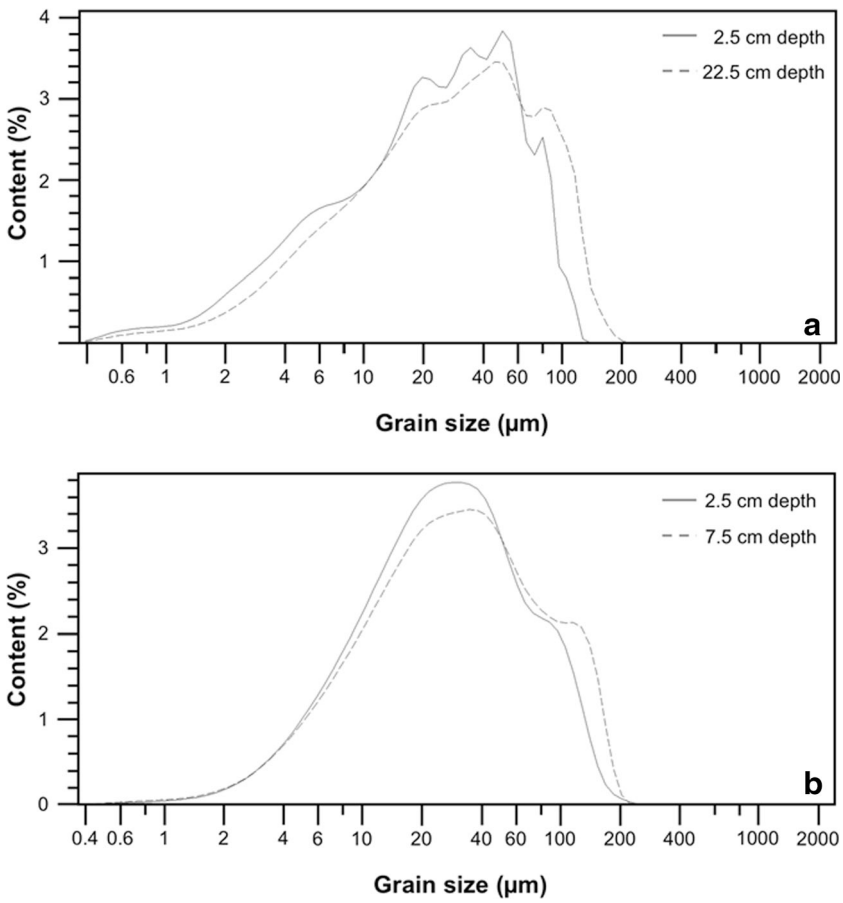

Fig. 4 Typical grain-size frequency distributions in different sediment samples from **a** the zone below microbial mats (zone AB) and **b** the zone without microbial mat development (zone CD)

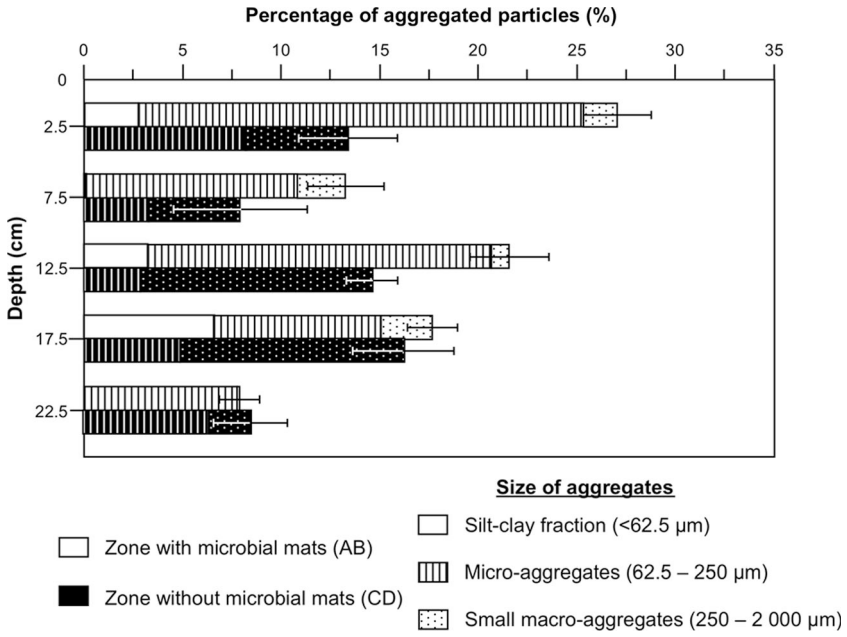

Fig. 5 Vertical variations of the percentage of aggregated particles collected in sediments below microbial mats (zone AB) and those not colonized by microbial mats (zone CD). The *bar spaces* represent the standard deviation of the relative percentages of aggregated particles. For each zone and depth, the relative percentages of the three different aggregate size fractions are also shown

the characterization of sediment sources, as well as their transport and deposition patterns (Folk and Ward 1957; Pedreros et al. 1996; Le Roux and Rojas 2007). The relationships between clay and sand percentages, MGS and sorting, and skewness and sorting distinguish the sediments below microbial mats (zone AB) from those not colonized by mats (zone CD) (Fig. 7a–c). Higher clay content and lower MGS indicate lower fluid flow velocity in zone AB, favoring the deposition of finer sediment particles. As this zone is closer to the lagoon edges and thus to the mangrove trees, complex root systems may play a dominant role in the dissipation of current and wave energy as well as in flow directions (Adame et al. 2010; Zhang et al. 2015). Moreover, the MGS decreases from the bottom to the top of sediments from the zone AB, below microbial mats (Table 2), indicating a decrease in current velocity over the past 20 years, probably linked to mangrove development throughout the lagoon (Crémière et al. submitted). In contrast, for sediments without surface microbial development (zone CD), the MGS shows higher values and remains fairly constant with depth, revealing that the tidal current velocity is higher and more constant through time. The lower values of sorting and the uni- or bi-modal symmetrical distribution observed in sediments without microbial mats are also in agreement with better sediment sorting in zone CD, probably due to the greater influence of tidal currents at this site further away from lagoon edges (Table 2 and Fig. 7b, c).

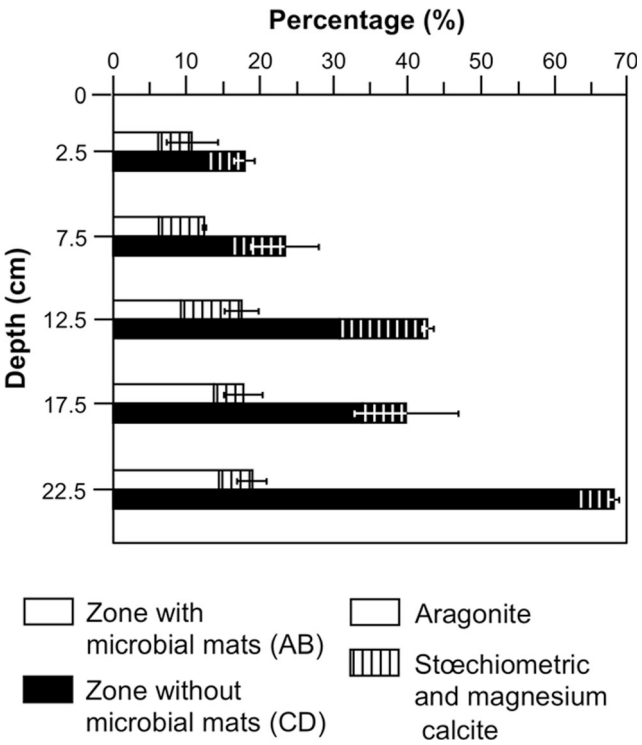

Fig. 6 Vertical repartition of the different carbonate phase (aragonite, calcite) contents of the two zones. The *bar spaces* represent the standard deviation in the total carbonate contents

In addition to these differences in grain-size distribution, the abundance of sedimentary particles involved in aggregate structures varies between the two zones (Table 2 and Fig. 5). These structures are formed by the agglomeration of mineral particles (i.e., clay, silt, and sand), depending on a variety of binding agents, such as roots, microbial polysaccharides, calcium bridges, and various (hydro) oxides (Tisdall and Oades 1982; Six et al. 2004). In this study, the percentage of aggregated particles shows a significant correlation with the percentage of clay and sand fractions (Pearson's correlation coefficient, $r_{\text{clay content}} = 0.596$, $r_{\text{sand content}} = -0.833$, $n = 10$, $P < 0.05$). These correlations indicate that sediment texture plays a key role in

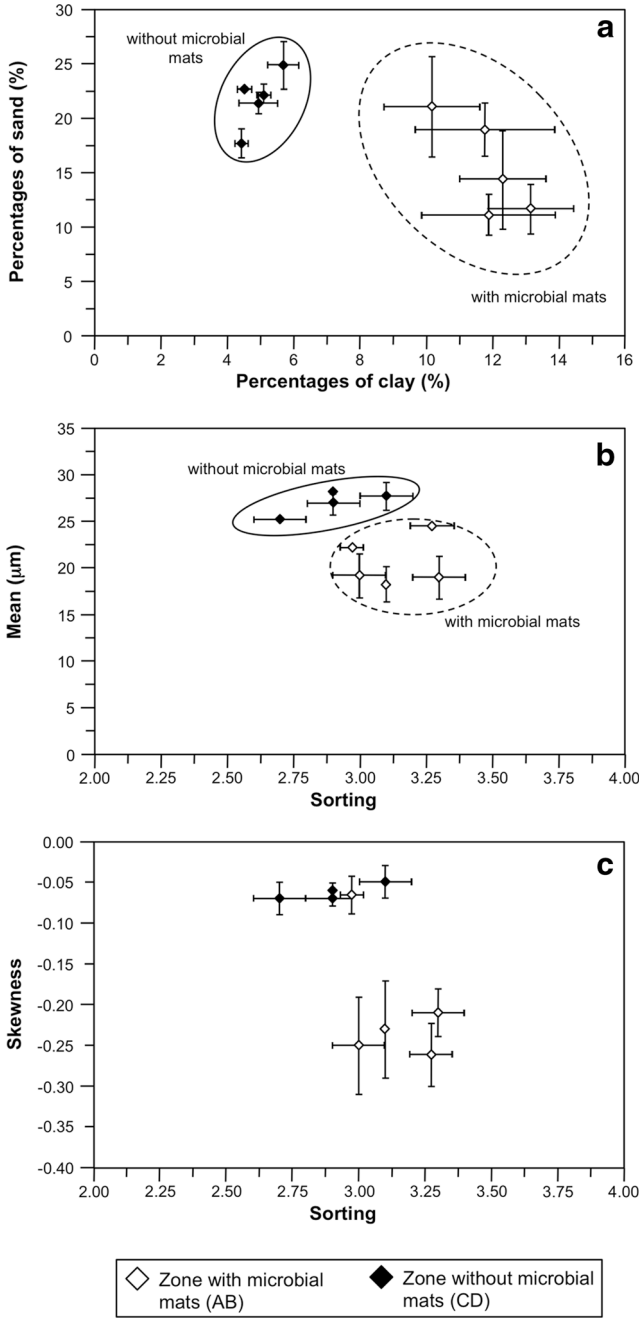

Fig. 7 Relationships between clay and sand contents (**a**), sorting and mean grain-size distribution (**b**), and sorting and skewness (**c**) of sediments from the two zones

aggregate formation, as previously shown by Tisdall and Oades (1982). Furthermore, TOC content is correlated with clay content and sand content (Pearson's correlation coefficient, $r_{\text{clay content}} = 0.733$, $r_{\text{sand content}} = -0.796$, $n = 10$, $P < 0.01$), indicating that muddy sediments are the primary vectors controlling sedimentary OM contents. Sediments below microbial mats (zone AB) are characterized by higher content of finer sediment particles, which is generally well correlated with higher mineral surface area (Mayer 1994; Goñi et al. 2003). This higher area might result in higher adsorption of OM onto mineral surfaces, forming a coverage of mineral surface that protects OM from microbial degradation and enhances aggregate formation. The higher TOC content observed in zone AB than in zone CD sediments increases even more the OC adsorption onto sediment particles and thus increases particle aggregation. The higher percentage of aggregated particles observed in the first 15 cm of depth in zone AB, characterized by microbial development, also indicates that the organic material released by mangrove tree roots and the EPS excreted by some of the micro-organisms forming microbial mats might both contribute to particle aggregation (Greenland et al. 1961).

The size of aggregate structures is also different in each of the two zones. In sediments below microbial mats, the relative percentage of the clay/silt-sized aggregate fraction was significantly higher below 10 cm deep, while that of micro-aggregate fraction was significantly higher above 15 cm depth (Fig. 5). Lower amounts of small macro-aggregates were always observed in these sediments, partly resulting from the penetrating effect of roots in macroporosity (Materechera et al. 1994). These differences in aggregate structure abundance and size observed between the two zones might result in variations of sediment structure inducing modifications in porewater movement, gas exchange, sedimentary OM dynamics, and nutrient cycling (Bronick and Lal 2005). In particular, aggregates might affect microbial capacity to access material bound in aggregates but also influence microbial community structure, limit oxygen diffusion, and determine nutrient absorption and desorption (Sexstone et al. 1995).

As carbonates are mostly of biogenic origin, the significant variations in total carbonate content and in the distribution of different carbonate phases between the two zones are linked to the dynamics of calcified biological communities. Higher values of total carbonate content in zone CD (Table 1 and Fig. 6) are probably linked to the occurrence of more favorable conditions for benthic organisms in sediments without microbial mats (Jean et al. 2015). Sediment grain size and TOC content might represent limiting factors for these communities, as exhibited by the significant relationship between them and the total carbonate content (Pearson's correlation coefficient, $r_{\text{clay content}} = -0.595$, $r_{\text{sand content}} = 0.694$, $r_{\text{TOC content}} = -0.955$, $n = 10$, $P < 0.05$). Furthermore, even if *Beggiatoa* mats are known to provide food for meiofauna and macrofauna (McHatton et al. 1996; Pascal et al. 2014), infauna can be influenced by the toxicity of these mat environments. In particular, *Beggiatoa* grow in sulfide-rich environments, which are toxic for many aerobic metazoans (Bagarinao 1992), and can create anoxic conditions by consuming up to 70 % of the total oxygen in sediment (Fenchel and Bernard 1995). The presence of high dissolved sulfide concentrations measured in pore waters from sediments below microbial mats and the absence of dissolved oxygen 2 cm above mats (Jean et al. 2015) are in agreement with the observation of pyrite. This mineral precipitates in environments, where reactive iron species

are available and hydrogen sulfide is produced due to microbial sulfate reduction under anoxic conditions (Berner 1972).

Sedimentary OM measured in the two zones shows lower TOC/TN ratios and higher $\delta^{13}C$ values than those reported earlier in superficial sediments of an adjacent *R. mangle* mangrove swamp located in the Grand Cul-de-Sac Marin in Guadeloupe (TOC/TN : 19 to 43, $\delta^{13}C$ values: -26.8 to -26.3 ‰; Lallier-Verges et al. 1998). This difference probably results from the fact that our study area is located within the Manche-à-Eau lagoon and thus receives higher OM inputs derived from marine phytoplankton. The $\delta^{13}C$ values show a strong negative correlation with the TOC content (Pearson's correlation coefficient, r = -0.911, n = 10, $P < 0.01$), indicating that sediments mainly receive OM derived from two potential sources. In the Manche-à-Eau lagoon, the two main potential OM sources are marine phytoplankton (which is the main component of the marine source) and C_3 terrestrial plants, mostly composed of *R. mangle*.

Assuming that diagenetic reactions do not significantly alter the OM $\delta^{13}C$ values and that the $\delta^{13}C$ values for each OM source are constant, it is possible to use the two end-member mixing equation based on these values and mass balance:

$$\delta^{13}C_{sed} = F_T \times \delta^{13}C_T + F_M \times \delta^{13}C_M \quad (1)$$

$$1 = F_T + F_M \quad (2)$$

where F_T and F_M are the fractions of terrestrial and marine OM, respectively. The $\delta^{13}C_{sed}$, $\delta^{13}C_T$, and $\delta^{13}C_M$ values represent the carbon isotopic composition of the sediment samples, the $\delta^{13}C$ value of *R. mangle* soft parts measured previously in an adjacent study site (-28.3 ± 0.3 ‰; Lallier-Verges et al. 1998), and the $\delta^{13}C$ value of marine phytoplankton end-members (-19.3 ± 0.8 ‰; Gearing et al. 1977; Jasper and Gagosian 1990), respectively. As TOC/TN ratios correlate very poorly with $\delta^{13}C$ (Pearson's correlation coefficient, $r_{[TOC/TN]\ ratio}$ = -0.347, n = 10, $P < 0.05$), they are not considered in the estimation of the terrestrial contribution to marine OM. This lack of correlation is probably due to the presence of a non-negligible amount of inorganic nitrogen bound to surface mineral particles, especially on the clay mineral species (Faganeli et al. 1991), and/or to the preferential remineralization of nitrogen relative to carbon by microbiologically mediated OM diagenesis (Hopkinson et al. 1997).

The calculated relative contributions shown in Fig. 8 varied from 59 ± 4 to 76 ± 3 % for *R. mangle* and from 24 ± 3 to 41 ± 4 % for marine phytoplankton. In all zones, sedimentary OM mainly originates from terrestrial plants. However, significantly higher percentages of sedimentary OM derived from marine phytoplankton are observed in sediments without microbial mats (mean of 38 ± 2 %) than in those with surface microbial development (mean of 28 ± 3 %). In sediments below microbial mats, the percentage of OM derived from terrestrial plants decreases slightly with depth, while it is quite stable in sediments without microbial mats. The calculated relative contribution of C_3 terrestrial plants to sedimentary OM is strongly correlated with the mean size of all sediments (Pearson's correlation coefficient, r_{mean} = -0.900, n = 10, $P < 0.01$). This contribution is also well correlated with skewness values for all sediments (Pearson's correlation coefficient, $r_{skewness}$ = -0.832, n = 10, $P < 0.01$). These correlations between grain-size parameters and the percentage of OM from terrestrial origin might indicate the influence of hydrodynamic effects on the accumulation of sedimentary OM in the study area. In particular, in sites closer to lagoon edges with microbial mats at the sediment-water interface, higher inputs of more refractory terrestrial OM might exist, due to the fact that mangrove debris is less regularly removed by the current and remains trapped by mangrove roots.

5 Conclusions

In the Manche-à-Eau lagoon, sediment characteristics in zones below colorless microbial mats and those not colonized by mats reveal significant differences. In particular, the grain-

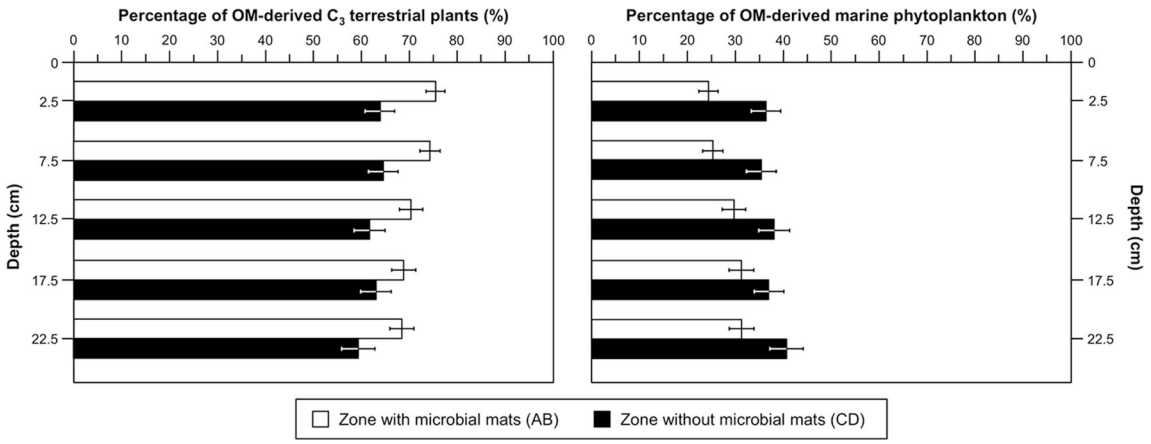

Fig. 8 Vertical variations of relative percentages of OM derived from the two potential sources, including C_3 terrestrial plants and marine phytoplankton, in the sediments from the two zones

size distribution of the sediment particles, the total carbonate content, and the $\delta^{13}C$ values seem to represent the main parameters correlated with the occurrence of microbial mats at the sediment-water interface. The abundance of carbonates, mainly corresponding to biogenic remains, shows a wide range of variation, probably linked to conditions in sediments without mats that are more favorable for benthic organisms. The variations in $[TOC/TN]_{atomic}$ ratios are mostly controlled by the presence of a non-negligible amount of inorganic nitrogen bound to surface clay mineral particles and/or by microbial processes.

The results of this study indicate that microbial mats grow at the surface of sediments characterized by lower MGS values and consequently with higher clay content. The deposition of greater amounts of fine sediment particles results from low hydrodynamic conditions favored by mangrove roots. These finer particles can be involved in aggregate structures, in particular when clay and TOC contents are higher. Aggregate formation may also be induced by the organic material released by mangrove roots and the EPS excreted by some of the micro-organisms forming the mats. These aggregates result in modifications of sedimentary OM dynamics and nutrient cycling. The input of more refractory OM derived from C_3 terrestrial plants seems to be greater in sediments below microbial mats. It probably results from the proximity of these sediments to the edges of the lagoon and the capacity of mangrove roots to avoid resuspension and removal of mangrove debris by currents. An increase in terrestrial OM inputs most likely induces an increase in the atomic TOC/TN ratios and a decrease in the $\delta^{13}C$ values of sedimentary OM. The abundant presence of pyrite in the sediments suggests a major contribution of sulfate reduction to the degradation of sedimentary OM. In the future, a better understanding of the role of microbial mats in OM degradation and thus in biogeochemical cycles might be achieved by coupling sediment characteristics with the characterization of dissolved inorganic components in pore waters and sulfur geochemistry.

Acknowledgments This work was financially supported by the Université Pierre et Marie Curie. The authors thank Omar Boudouma for performing the SEM observations and EDS. The authors are also grateful to Jessy Toncin for her assistance with the mineralogical and OM geochemical analyses. They also wish to thank Laurent Brutier and Michel Lareal (LOG, Wimereux, France) for their technical assistance. Fruitful comments and constructive suggestions by two anonymous reviewers considerably helped to improve the manuscript. The authors also wish to thank Carmela Chateau Smith for the assistance with English.

References

Adame MF, Neil D, Wright SF, Loverlock CE (2010) Sedimentation within and among mangrove forests along a gradient of geomorphological settings. Estuar Coast Shelf Sci 86:21–30

Al-Thukair AA, Abed RMM, Mohamed L (2007) Microbial community of cyanobacteria mats in the intertidal zone of oil-polluted coast of Saudi Arabia. Mar Pollut Bull 54:173–179

Bagarinao T (1992) Sulfide as an environmental factor and toxicant: tolerance and adaptations in aquatic organisms. Aqua. Toxicol 24:21–62

Berner RA (1972) Sulfate reduction, pyrite formation and the oceanic sulfur budget. Nobel Symposium 20:347–362

Blott SJ, Pye K (2001) GRADISTAT: a grain size distribution and statistics package for the analysis of unconsolidated sediments. Earth Surf Proc Land 26:1237–1248

Bouillon S, Connolly RM, Lee SY (2008) Organic matter exchange and cycling in mangrove ecosystems: recent insights from stable isotope studies. J Sea Res 59:44–58

Bronick CJ, Lal R (2005) Soil structure and management: a review. Geoderma 124:3–22

Canfield DE, Des Marais DJ (1993) Biogeochemical cycles of carbon, sulfur, and free oxygen in a microbial mat. Geochim. Cosmochim Acta 57:3971–3984

Crémière A, Strauss H, Sebilo M, Hong W-H, Laverman AM, Gros O, Toncin J, Henry F, Gontharet S (submitted). Sulfur diagenesis under rapid accumulation of organic-rich sediments in a marine mangrove from Guadeloupe (French West Indies). Submitted to Chemical Geology

Decho AW (1990) Microbial exopolymer secretions in ocean environments: their role(s) in food webs and marine processes. Oceanogr. Mar Biol Annu Rev 28:73–153

Delfino DO, Wanderley MD, e SilvaSilva LH, Feder F, Lopes FAS (2012) Sedimentology and temporal distribution of microbial mats from Brejo do Espinho, Rio de Janeira, Brazil. Sediment Geol 263-264:85–95

Faganeli J, Planinc R, Pezdic J, Smodis B, Stegnar P, Ogorelec B (1991) Marine geology of the Gulf of Trieste (northern Adriatic) geochemical aspects. Mar Geol 99:93–103

Fenchel T, Bernard C (1995) Mats of colourless sulphur bacteria. *I. major* Microbial processes. Mar Ecol Prog Ser 128:161–170

Folk RL (1954) The distinction between grain size and mineral composition in sedimentary rock nomenclature. J Geol 62:344–359

Folk RL, Ward WC (1957) Brazos River bar: a study in the significance of grain size parameters. J Sediment Petrol 27:3–26

Gearing P, Plucker FE, Parker PL (1977) Organic carbon stable isotope ratios of continental margin sediments. Mar Chem 5:251–266

Goñi MA, Ruttemberg KC, Eglinton TI (1998) A reassessment of the sources and importance of land-derived organic matter in surface sediments from the Gulf of Mexico. Geochim Cosmochim Acta 62:3055–3075

Goñi MA, Teixeira MJ, Perkey DW (2003) Sources and distribution of organic matter in a river-dominated estuary (Winyah Bay, SC, USA. Estuar Coast Shelf S 57:1023–1048

Greenland DJ, Lindstrom GR, Quirk JP (1961) Role of polysaccharides in stabilization of natural soil aggregates. Nature 191:1283–1284

Guidi-Rontani C, Jean MNR, Gonzalez-Rizzo S, Bolte-Kluge S, Gros O (2014) Description of new filamentous toxic cyanobacteria (*Oscillatoriales*) colonizing sulphidic periphyton mat in marine mangrove. FEMS Microbiol Lett 359(2):173–181

Guilcher A, Marec A (1978) Le récif-barrière et le lagoon du Grand Cul-de-Sac Marin (Guadeloupe, Antilles françaises). Géomorphologie et sediments. Oceanol Acta 1(4):435–444

Hopkinson CS, Fry B, Nolin AL (1997) Stoichiometric of dissolved organic matter dynamics on the continental shelf of the northeastern USA. Cont Shelf Res 17:473–489

Jasper JP, Gagosian RB (1990) The sources and deposition of organic matter in the late quaternary Pigmy Basin, Gulf of Mexico. Geochim Cosmochim Acta 54:1117–1132

Jean MRN, Gonzalez-Rizzo S, Gauffre-Autelin P, Lengger SK, Schouten S, Gros O (2015) Two new *Beggiatoa* species inhabiting marine mangrove sediments in the Carribean. PLoS One 10(2):e0117832

Jennerjahn TC, Itterkkot V (2002) Relevance of mangroves for the production and deposition of organic matter along tropical continental margins. Naturwissenschaften 89:23–30

Lallier-Verges L, Parrussel BP, Disnar J-R, Baltzer F (1998) Relationships between environmental conditions and the diagenetic evolution of organic matter derived from higher plants in a modern mangrove swamp system (Guadeloupe, French West Indies. Org Geochem 29: 1663–1686

Le Roux JP, Rojas EM (2007) Sediment transport patterns determined from grain size parameters: overview and state of the art. Sediment Geol 202:473–488

Mantran M, Hamparian R, Bouchereau J-L (2009) Géomorphologie et hydrologie de la lagune de la Manche-à-eau (Guadeloupe, Antilles françaises); geomorphology and hydrology of the Manche-à-eau lagoon (Guadeloupe, French West Indies). Géomorphologie Relief Processus Environ 3:199–210. doi:10.4000/geomorphologie.7606

Materechera SA, Kirby JM, Alston AM, Dexter AR (1994) Modification of soil aggregation by watering regime and roots growing through beds of large aggregates. Plant Soil 160:57–66

Mayer LM (1994) Surface area control of organic matter accumulation in continental shelf sediments. Geochim Cosmochim Acta 58:1271–1284

McHatton SC, Barry JP, Jannasch HW, Nelson DC (1996) High nitrate concentrations in vacuolated, autotrophic marine *Beggiatoa* spp. App Environ Microbiol 62:954–958

Meysman FJR, Risgaard-Petersen N, Malkin SY, Nielsen LP (2015) The geochemical fingerprint of microbial long-distance electron transport in the seafloor. Geochim Cosmochim Acta 152:122–142

Pascal P-Y, Dubois S, Boschker HTS, Gros O (2014) Trophic role of large benthic sulfur bacteria in mangrove sediment. Mar Ecol Prog Ser 516:127–138

Pedreros R, Howa HL, Michel D (1996) Application of grain size trend analysis for the determination of sediment transport pathways in intertidal areas. Mar Geol 135:35–49

Seckbach J, Oren A (2010) Microbial mats. Modern and ancient microorganisms in stratified systems. Springer, New York

Sexstone AJ, Revsbech NP, Parkin TB, Tiedje JM (1995) Direct measurement of oxygen profiles and denitrification rates in soil aggregates. Soil Sci Soc Am J 49:645–651

Six J, Bossuyt H, Degryze S, Denef K (2004) A history of research on the link between (micro)aggregates, soil biota, and soil organic matter dynamics. Soil Till Res 79:7–31

Stal LJ (2010) Microphytobenthos as biogeomorphological force in intertidal sediment stabilization. Ecol Eng 36:236–245

Stolz J (2000) Structure of microbial mats and biofilms. In: Riding RE, Awramik SM (eds) Microbial sediments. Springer, Berlin, pp. 1–8

Tisdall J, Oades J (1982) Organic matter and water-stable aggregates in soils. J Soil Sci 33:141–163

van Gemerden H (1993) Microbial mats-a joint venture. Mar Geol 113:3–25

Wentworth CK (1922) A scale of grade and class terms for clastic sediments. J Geol 30:377–392

Zhang X, Cha VP, Cheong H-F (2015) Hydrodynamics in mangrove prop roots and their physical properties. J Hydro Environ Res 9:281–294